Experimental Study of the Evolution of the Breach and the Discharge through the Breach Resulting from Piping Due to Seepage at the Mid-part of Earthfill Dam

M. Sukru Guney [1], Emre Dumlu[2*], and Merve Okan[1]
[1] Civil Engineering Department, Izmir University of Economics, Izmir, Turkey;
Email: sukru.guney@ieu.edu.tr (M.S.G.), merve.okan@ieu.edu.tr (M.O.)
[2] National Center for Computational Hydroscience and Engineering, University of Mississippi, Oxford, MS, USA
*Correspondence: edumlu@go.olemiss.edu (E.D.)

***Abstract*—One of the main factors that leads to earth-fill dam failures is the internal erosion, commonly referred to as piping. Regarding the geometry of the breach and the discharge of water flowing through the breach, many researchers working with numerical analyses in this field make some simplified assumptions. This study was carried out as a part of the project supported by the Turkish Council for Scientific and Technological Research (TUBITAK) and it includes experimental research with the goal of supplying the data required to carry out numerical analysis using more realistic approaches. A dam with a height of 65 cm, a bottom width of 200 cm and a crest width of 5 cm was built in a flume 1 m wide, 0.81 m high and 6.14 m long. Before the construction of the dam, some common soil mechanics tests were carried out. The dam was constructed by using a mixture consisting of 85 % fine sand and 15% clay. In order to generate the formation of the breach, a square shaped rock salt layer of 2 cm side lying from upstream to downstream was placed at 28 cm from the bottom of the dam body. The progression of the dam failure was captured by six cameras located at different locations. Gauss Area formula was applied to determine the time-varied breach areas at upstream and downstream sides. The discharge of water through the breach and average flow velocity were determined by using the continuity equation. The changes in water depth in the channel were also recorded. The experimental findings continue to be compared with numerical results obtained from the software PLAXIS 3D.**

***Keywords*—earth-fill dam, piping, breach geometry, breach development, discharge through breach**

I. Introduction

Piping is one of main causes of earth-fill dam failures. Soil erosion in earth structures, particularly in earth dams and levees, might occur through embankment, foundation or from embankment to foundation. This kind of erosion has phases: a) initiation and continuation of erosion, b) progression to form a pipe, and c) formation of a breach [1]. The evolution of breach resulting from piping is an important issue in experimental and numerical investigation concerning embankment dam failure. The FP5 IMPACT (Investigation of Extreme Flood Process and Uncertainty) European project (2001–2004) addressed the assessment and reduction of risks from extreme flooding caused by natural events or the failure of dams and flood defence structures [2]. Research had been undertaken through a combination of laboratory physical modelling, field data collection, field testing, theoretical studies, and numerical simulations. There exist many studies about dam failures especially because of overtopping in the literature, however since it is relatively difficult to observe erosion process and conduct controlled experiments, there are not too much survey about dam failure due to piping [3]–[5]. Chen, Zhong and Shen [4] indicated that between 1954 and 2018, 3541 dam breach accidents occurred and more than 30% of them was due to piping. Greco, Pontillo, Iervolino and Leopardi [6] simulated the evolution of a breach in an earth-fill dam by means of a two-dimensional depth-averaged (2DH) numerical model, from both the conceptual and the numerical point of view. Sharif, Elkholy, Hanif Chaudhry and Imran [3] constructed a dam 15 cm high in a laboratory flume by using a mixture of sand, silt, and clay with different compaction rates and examined the changes in the depth, area, and volume of erosion during the piping evolution by utilizing an image processing technique. Most of the researchers realizing numerical analyses make some simplified assumptions concerning shape of a breach and discharge of water flowing through the breach. Morris *et al.* [7] revealed that instead of simplified approaches, more realistic approaches are required about the breach mechanism as well as the breach geometry and flow through the breach. Zhu, Visser, Vrijling, and Wang [8] investigated experimentally the breaching of embankments. ASCE/EWRI Task Committee [9] made a publication about earthen embankment breaching (2011). Froehlich [10] presented two nonlinear mathematical models to predict peak discharge. Wang, *et al.* [11] proposed empirical and semi-analytical models for predicting peak outflows caused by embankment dam failures. Ashraf,

Manuscript received July 30, 2022; revised August 25, 2022; accepted September 5, 2022.

et al. [12] studied the breach parameters by using large scale physical modelling and statistical methods. Tian, *et al.* [13] investigated experimentally formation and evolution characteristics of dam breach and tailing flow from dam failure.

This study is a part of the project 119M609 supported by the Scientific and Technological Research Council of Turkey. The aim of this study is first to realize the experiments to study the evolution of dam failure resulting from piping along the centerline at 37 cm below the crest of the earth-fill dam, and then evaluate the experimental findings by using the software package PLAXIS-3D.

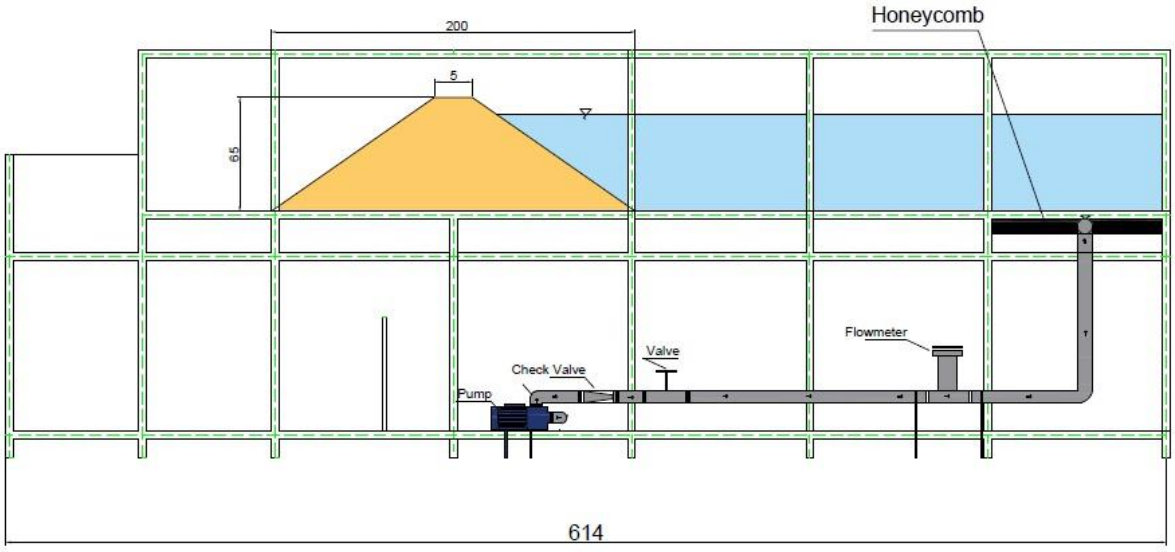

Figure 1. Experimental flume.

II. Experimental Procedure

A dam 65 cm high was constructed in a rectangular channel of a flume 1 m wide, 0.81 m high and 6.1 m long (Fig. 1). The bottom width of the homogeneous dam was 200 cm, and its crest width was 5 cm with the upstream and downstream slope of 1:1.5. Water was circulated between the lower reservoir and the upper channel by means of a pump.

Some soil mechanics experiments were carried out before building the dam. The soil mixture utilized at the construction of the dam was prepared by using 85% fine sand and 15% clay. The grain-size distribution of the mixture obtained from the wet sieve analyses is shown in Fig. 2.

From Fig. 2, some characteristic diameters were obtained as D_{10}= 0.078 mm, D_{30}= 0.13 mm, D_{50}= 0.17 mm, and D_{60}= 0.21 mm. The uniformity coefficient C_u equals 2.69 and the curvature coefficient C_c is equal to 1.03.

The specific weight of the mixture was found to be as G_s = 2.67, from the test ASTM D854–14.

The permeability of the mixture was found as k= 1.18×10^{-3} cm/s from the falling head permeability test.

The standard proctor tests (ASTM-698) were performed by applying both 13 and 25 blows, and the so obtained curves are plotted in Fig. 3 and Fig. 4, respectively. The maximum dry density and optimum water content were obtained as Υ_{drymax}= 1.653 g/cm^3 and w_{opt} = 15.4% from the test with 13 blows and as Υ_{drymax}= 1.694 g/cm^3 and w_{opt} = 13.6% from the 25 blows test.

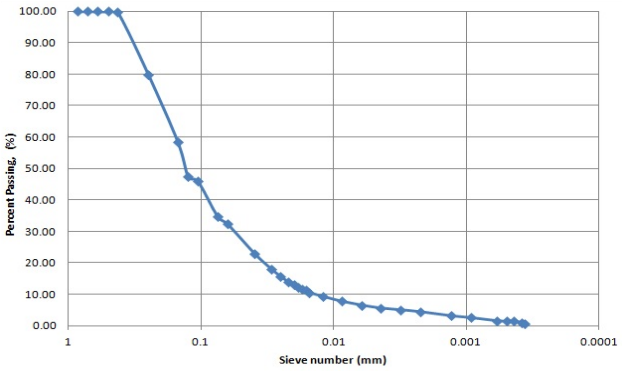

Figure 2. Grain size distribution of the dam material.

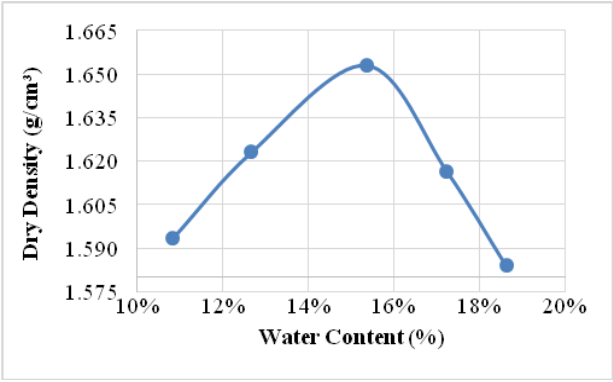

Figure 3. Standard proctor test with 13 blows.

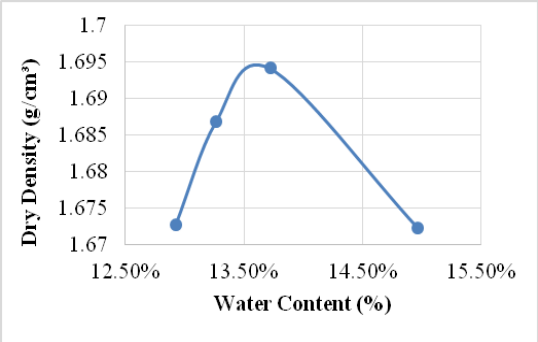

Figure 4. Standard proctor test with 25 blows.

Some construction stages and completed shape of the dam body are shown in Fig. 5. The dam was constructed layer by layer, the initial six layers being 10 cm and last layer 5 cm thick. After placement of the soil material, the mixture was compacted using a flat plate and a proctor hammer (Fig. 5a). When the compaction was completed, the molds were extracted, and then the sides of the dam were trimmed by using a trowel.

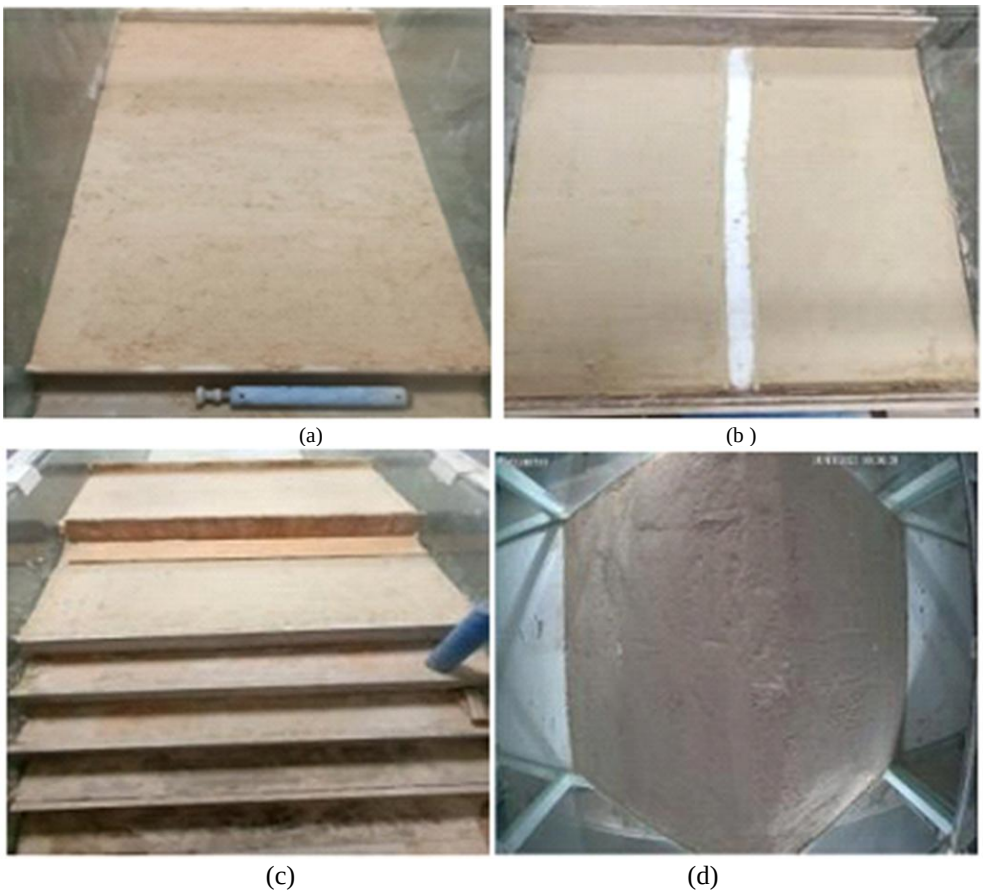

Figure 5. Some construction stages a) the compacted first layer, b) the weak zone of rock salt at 28 cm from the bottom, c) compaction of the fifth layer, d) the final shape of the dam

The flow rate was measured by a magnetic flowmeter. The evolution of the dam failure was recorded by six cameras placed at different locations. In order to adjust the water level, an electromagnetic sensor was mounted. This sensor started and stopped the pump when water depths in the channel were 0.60 m and 0.615 m, respectively.

In order to generate the formation of the breach, a square shaped rock salt layer of 2 cm side lying from upstream to downstream was placed at 28 cm from the bottom of the dam body.

III. Experimental Findings

The experiments were carried out twice in order to check the repeatability [14].

The temporal developments of the breach concerning the first experiment and recorded by the cameras located at downstream and upstream of the dam are given in Fig. 6 to 12. The time t=0 corresponds to the commencement of the piping.

The records concerning the first and second experiments were found to be similar to each other. Therefore, the reliability of the experiment was satisfied.

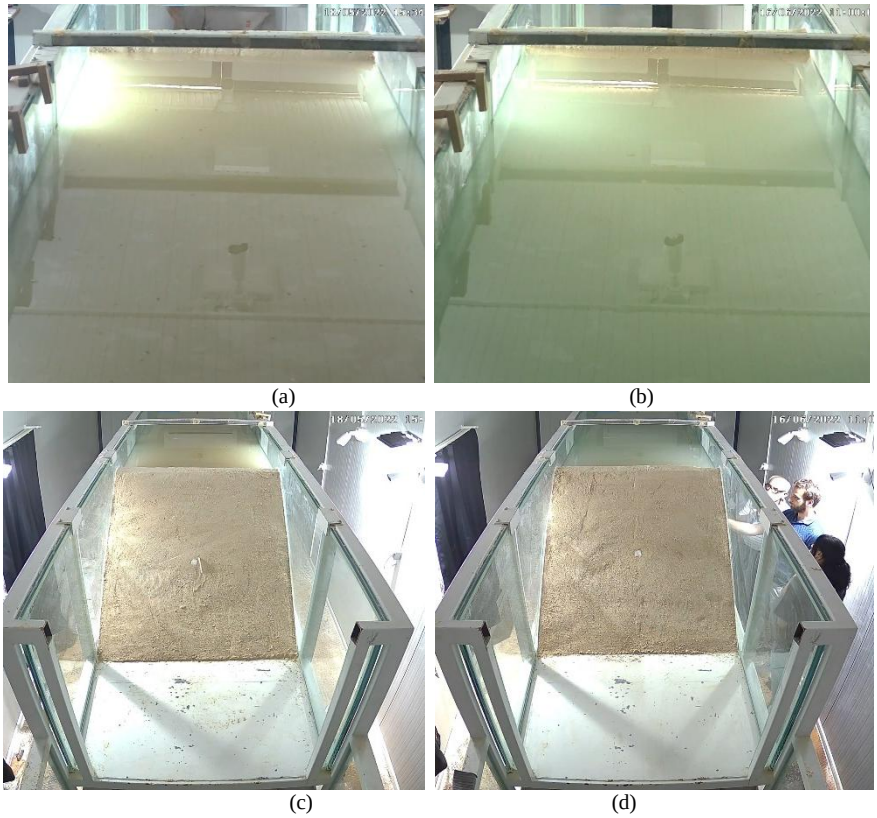

(a) (b)

(c) (d)

Figure 6. The temporal developments of the breach in both dams at t=0 s a) upstream of the first dam, b) upstream of the second dam, c) downstream of the first dam, d) downstream of the second dam.

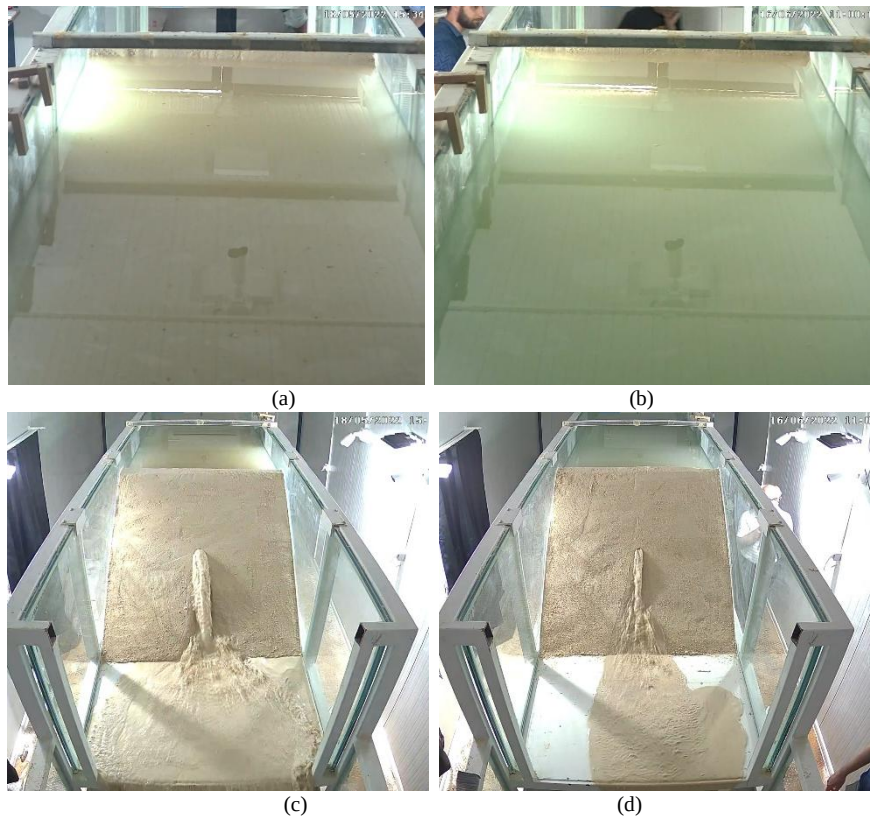

(a) (b)

(c) (d)

Figure 7. The temporal developments of the breach in both dams at t=15 s a) upstream of the first dam, b) upstream of the second dam, c) downstream of the first dam, d) downstream of the second dam.

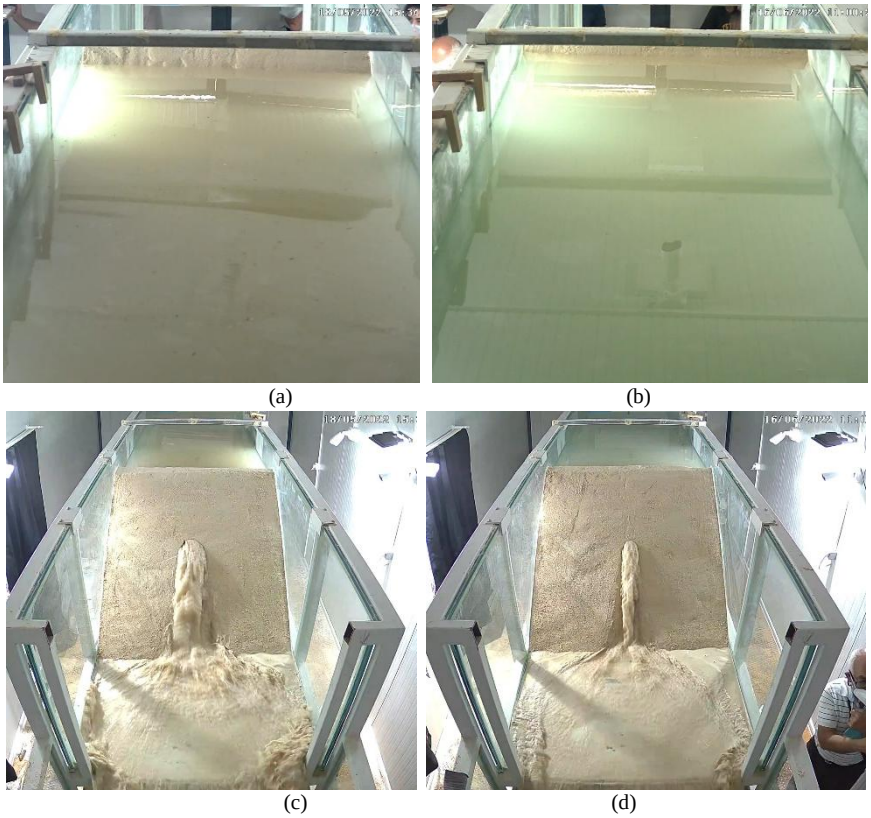

(a) (b)

(c) (d)

Figure 8. The temporal developments of the breach in both dams at t=25 s a) upstream of the first dam, b) upstream of the second dam, c) downstream of the first dam, d) downstream of the second dam.

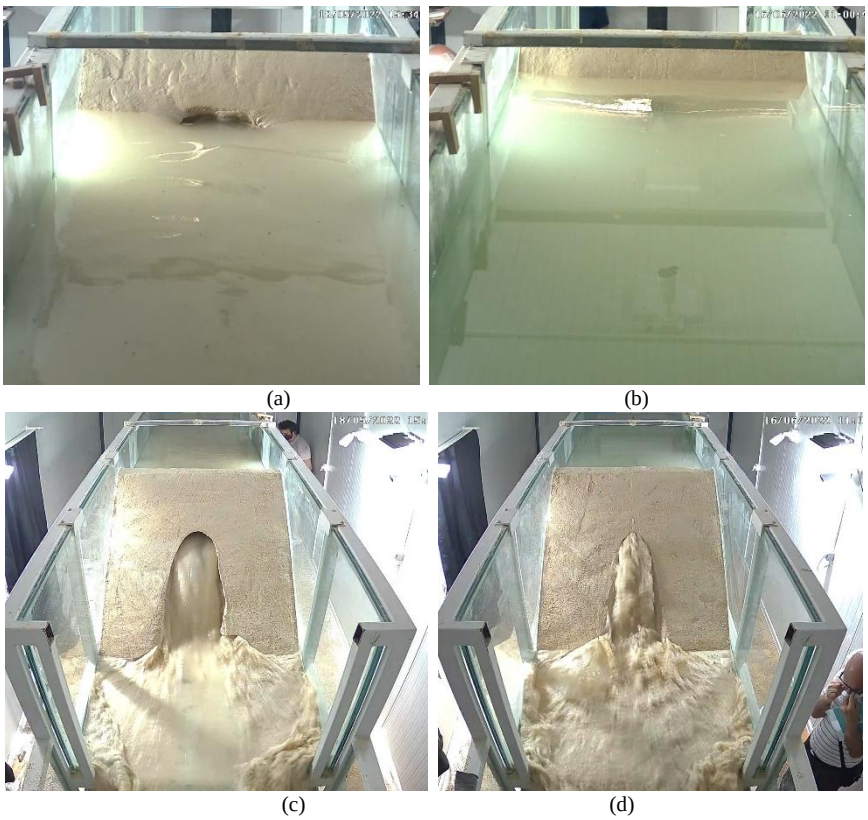

(a) (b)

(c) (d)

Figure 9. The temporal developments of the breach in both dams at t=40 s a) upstream of the first dam, b) upstream of the second dam, c) downstream of the first dam, d) downstream of the second dam.

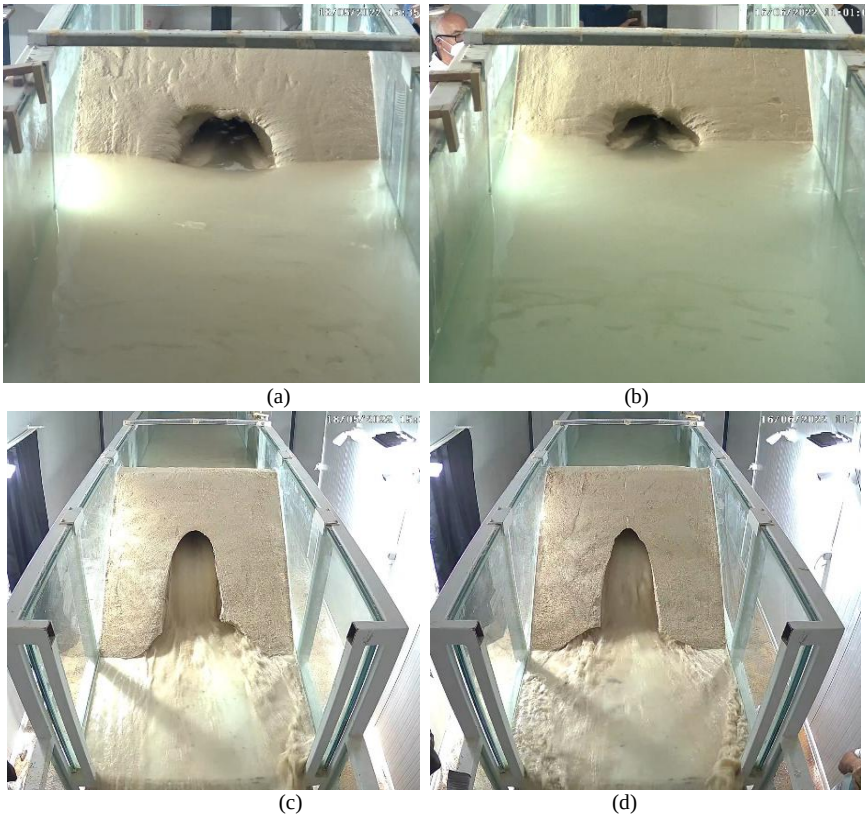

(a) (b)

(c) (d)

Figure 10. The temporal developments of the breach in both dams at t=60 s a) upstream of the first dam, b) upstream of the second dam, c) downstream of the first dam, d) downstream of the second dam.

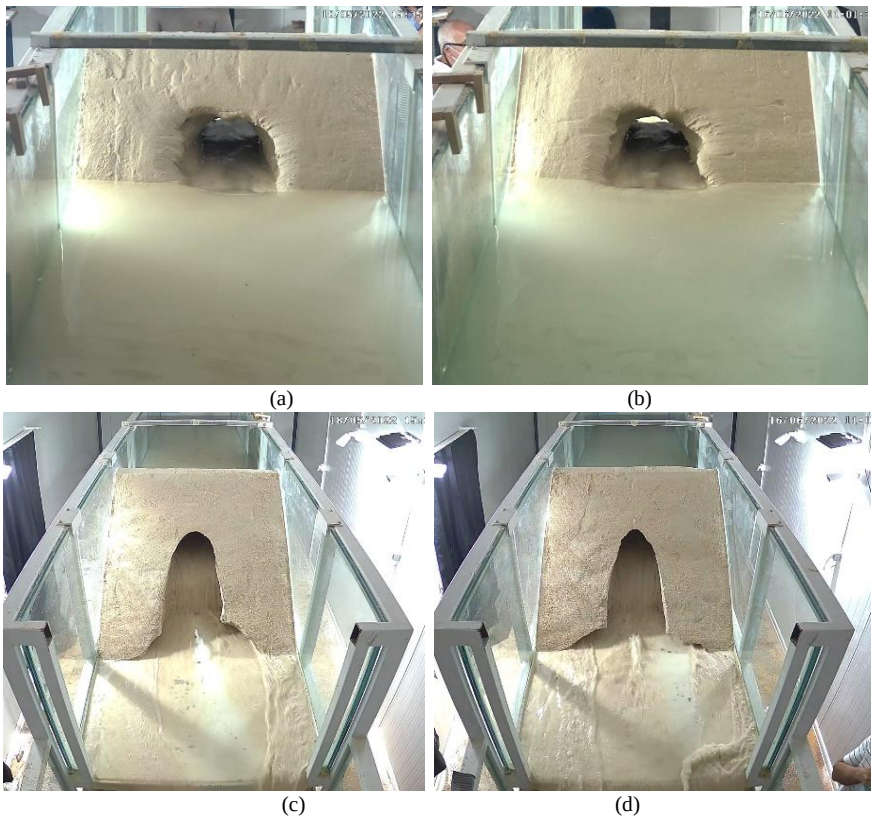

(a) (b)

(c) (d)

Figure 11. The temporal developments of the breach in both dams at t=90 s a) upstream of the first dam, b) upstream of the second dam, c) downstream of the first dam, d) downstream of the second dam.

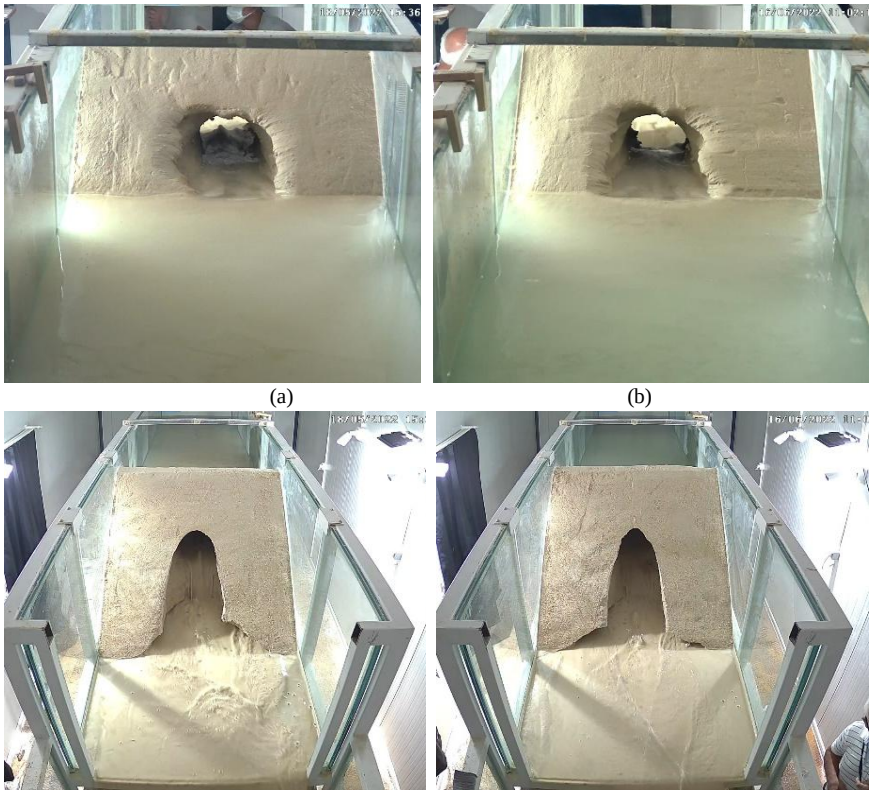

Figure 12. The temporal developments of the breach in both dams at t=134 s a) upstream of the first dam, b) upstream of the second dam, c) downstream of the first dam, d) downstream of the second dam.

The time-dependent water depths in the channel were also recorded.

In order to evaluate the shape of the breach and determine the changes in its geometry, the upstream and downstream cameras records were analysed. For the purpose of improving fisheye images, the videos taken from lateral camera records were edited and straightened with Hit-film-Express version 2021.1. Moreover, extra sensitive solutions were implemented to ensure that the images are completely flat. The images taken from the records were scaled and the boundary coordinates of the breaches at downstream and upstream sides were specified at Get-data Graph Digitizer 2.26 software. The breach areas corresponding to different instants were computed by the Gauss Area functions.

The discharge of water through the breach was determined by using the continuity equation.

$$\Delta S = (Q_{pump} - Q_{breach}) \cdot \Delta t \quad (1)$$

where Q_{pump} is the flow rate delivered by the pump, Q_{breach} is the discharge through the breach, ΔS is the storage change in the channel during the time interval Δt. The average velocity V of the flow through the breach was approximately calculated by using the Eq. (2).

$$V = Q_{breach} / A \quad (2)$$

where A represents wetted area.

The temporal water depths in the channel and discharge through the breach calculated by Eq. (1) are given in Fig. 13 and Fig. 14, respectively.

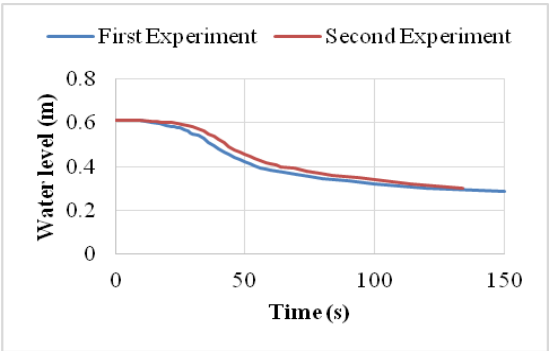

Figure 13. Time-varied water depths in channel.

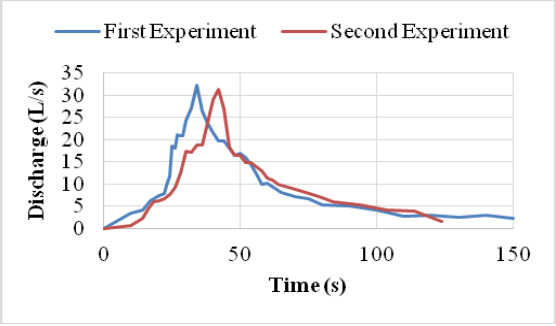

Figure 14. Time-varied discharges through the breach.

The temporal variations of the breach area at upstream and downstream are shown in the Fig. 15.

The time dependent wetted area and velocity values obtained by using Eq. (2) at upstream and downstream are given in Fig. 16 and Fig. 17, respectively.

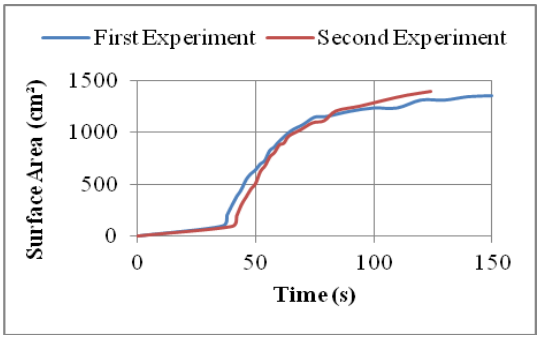

(a)

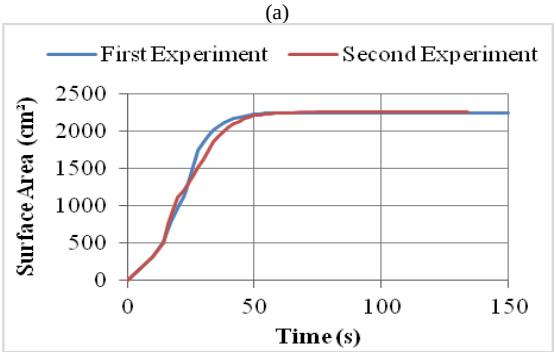

(b)

Figure 15. Temporal variations of the breach area (a) at upstream and (b) at downstream.

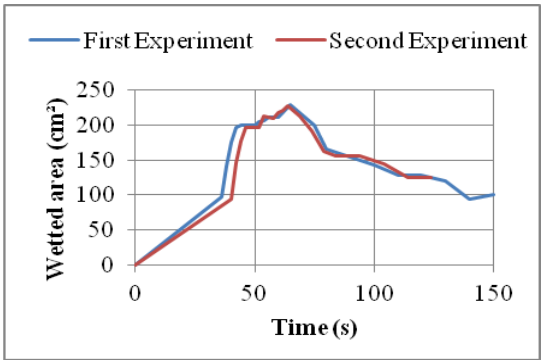

(a)

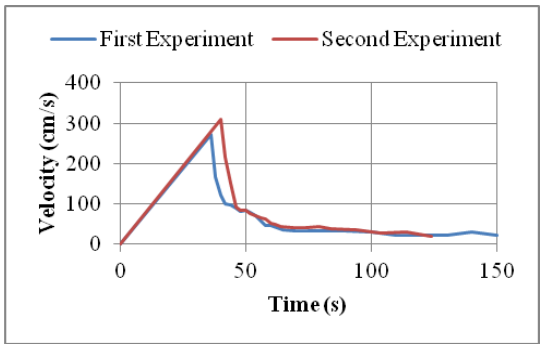

(b)

Figure 16. (a) Wetted area and (b) velocity values at upstream

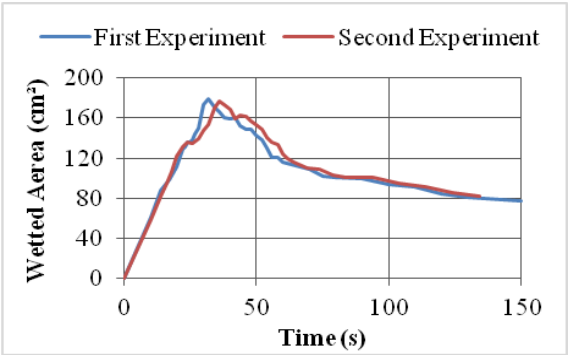

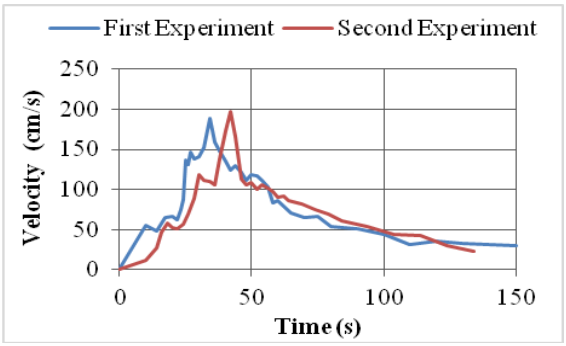

Figure 17. (a) Wetted area and (b) velocity values at downstream

IV. Results and Discussion

In this study, the time-varied evolution of the breach resulting from the piping at the middle part of an earth-fill dam was investigated experimentally and the values of some measured parameters are given in Table I.

TABLE I. Values of Some Experimental Findings

Parameters	Experiment 1	Experiment 2	Average
Q_{max} (L/s)	32.38 (at t=34 s)	31.33 (at t=42 s)	31.855
$A_{maxbreach\text{-}ups}$ (cm^2)	1361.1 (at t=150 s)	1398.8 (at t=124)	1379.95
$A_{maxbreach\text{-}down}$ (cm^2)	2248.9 (at t=60 s)	2250.2 (at t=69 s)	2249.55
$A_{maxwet\text{-}ups}$ (cm^2)	228.9 (at t=65 s)	227.1 (at t=64 s)	228
$A_{maxwet\text{-}down}$ (cm^2)	178.7 (at t=32 s)	176.7 (at t=36 s)	177.7
$V_{maxwet\text{-}ups}$ (cm/s)	271.3 (at t=36 s)	310.4 (at t=40 s)	290.85
$V_{maxwet\text{-}down}$ (cm/s)	189.3 (at t=34 s)	196.9 (at t=42 s)	193.1

The discharges through the breach corresponding to different instants were calculated using the continuity equation. The boundary coordinates of the breach surface areas and wet areas of the breach were obtained by using the Get-Data Graph Digitizer, and the areas at each time were calculated by applying the Gauss-area function of the obtained coordinates. The time dependent velocity values through the breach areas were also calculated.

V. Conclusion

The experiments were realized twice in order to check the repeatability. It was revealed that the compatibility between the measures of two experiments is acceptable.

The time-dependent discharges values obtained from the experiments formed a hydrograph similar to a common flood hydrograph.

During the experiment, the breach initiated at the downstream side and then evolved towards the upstream side. The change in the breach area was very small until the peak flow rate was reached. Beyond this time, the breach surface area at downstream side remained almost constant while the breach area continued to increase at upstream side. The final value of the breach area was nearly twice at downstream side compared to that at upstream side.

The experimental findings were also compared with numerical results obtained from the software PLAXIS 3D. The numerical analysis was performed in both steady and unsteady conditions. The accord between experimental and numerical results was found to be fairly good.

Some other experiments concerning the piping in both homogeneous and clay-cored earthen dams were also carried out with different scenarios, according to the location of the weak layer. The results of the experiments performed in the scope of the project supported by the Turkish Scientific and Technological Research Council continue to be evaluated and compared.

Conflict of Interest

The authors declare no conflict of interest.

Author Contributions

Emre Dumlu together with Merve Okan carried out the soil mechanics experiments, realized the construction of the dam, performed the piping experiments, analyzed the camera records, and performed the required calculations. Afterward, Emre Dumlu performed the numerical analysis in both steady and unsteady conditions. M. Sukru Guney supervised the entire study and wrote the paper; all authors had approved the final version.

Funding

The research is financially supported by the Scientific and Technological Research Council of Turkey (TUBITAK) through the project 119M609.

References

[1] R. Fell, C. H. Wan, and M. Foster, "Progress report on methods for estimating the probability of failure of embankment dams by internal erosion and piping," University of New South Wales, Sydney, Australia, 2003.

[2] Y. Zech and S. Soares-Fraz ão, "Dam-break flow experiments and real-case data. A database from the European IMPACT research," *J. Hydraul. Res.*, vol. 45, no. SPEC. ISS., pp. 5–7, 2007.

[3] Y. A. Sharif, M. Elkholy, M. Hanif Chaudhry, and J. Imran, "Experimental study on the piping erosion process in earthen embankments," *J. Hydraul. Eng.*, vol. 141, no. 7, p. 04015012, 2015.

[4] S. Shui Chen, Q. Ming Zhong, and G. Ze Shen, "Numerical modelling of earthen dam breach due to piping failure," *Water Sci. Eng.*, vol. 12, no. 3, pp. 169–178, 2019.

[5] M. Elkholy, Y. A. Sharif, M. H. Chaudhry, and J. Imran, "Effect of soil composition on piping erosion of earthen levees," *J. Hydraul. Res.*, vol. 53, no. 4, pp. 478–487, 2015.

[6] M. Greco, M. Pontillo, M. Iervolino, and A. Leopardi, "2DH numerical simulation of breach evolution in an earth dam," in *Proc. River-flow2008*, 2008, vol. 1, pp. 661–667.

[7] M. Morris, M. Hassan, A. Kortenhaus, P. Geisenhainer, P. Visser, and Y. Zhu, "Modelling breach initiation and growth," *Flood Risk Manag. Res. Pract.*, pp. 581–591, Oct. 2008.

[8] Y. Zhu, P. J. Visser, J. K. Vrijling, and G. Wang, "Experimental investigation on breaching of embankments," *Sci. China Technol. Sci.*, vol. 54, no. 1, pp. 148–155, 2011.

[9] The ASCE/EWRI Task Committee on Dam/Levee Breaching (Break Fluvial Processes). / Earthen embankment breaching. In: Journal of Hydraulic Engineering. 2011; vol. 137, no. 12. pp. 1549-1564.

[10] D. C. Froehlich, "Predicting peak discharge from gradually breached embankment dam," *J. Hydrol. Eng.*, vol. 21, no. 11, pp. 04016041_1 - 04016041_15, 2016.

[11] B. Wang, Y. Chen, C. Wu, Y. Peng, "Empirical and semi-analytical models for predicting peak outflows caused by embankment dam failures," *J. Hydrol.*, vol. 562, no. May, pp. 692–702, 2018.

[12] M. Ashraf, A. H. Soliman, E. El-Ghorab, and A. El Zawahry, "Assessment of embankment dams breaching using large scale physical modelling and statistical methods," *Water Sci.*, vol. 32, no. 2, pp. 362–379, 2018.

[13] S. Tian, X. Dai, G. Wang, Y. Lu, and J. Chen, "Formation and evolution characteristics of dam breach and tailings flow from dam failure: an experimental study," *Nat. Hazards*, vol. 107, no. 2, pp. 1621–1638, 2021.

[14] E. Dumlu, (2022, December 1). Experimental and numerical investigation of the evolution of piping and resulting breach in earth-fill dams. GCRIS Database | Izmir Institute of Technology. https://gcris.iyte.edu.tr/handle/11147/13269